JACS
JOURNAL OF THE AMERICAN CHEMICAL SOCIETY
pubs.acs.org/JACS
Article

Observation of the Protein-Inorganic Interface of Ferritin by Cryo-Electron Microscopy

Sagnik Sen, Amar Thaker, Alison Haymaker, Dewight Williams, Po-Lin Chiu, and Brent L. Nannenga*

Cite This: J. Am. Chem. Soc. 2025, 147, 3333−3340
Read Online

Chemical Engineering, School for Engineering of Matter, Transport and Energy, Arizona State University, Tempe, AZ 85287, United States
Biodesign Center for Applied Structural Discovery, Biodesign Institute, Arizona State University, 727 East Tyler Street, Tempe, AZ 85281, United States
John M. Cowley Center for High Resolution Electron Microscopy, Arizona State University, Tempe, AZ 85287, United States
School of Molecular Sciences, Arizona State University, Tempe, AZ 85287, United States

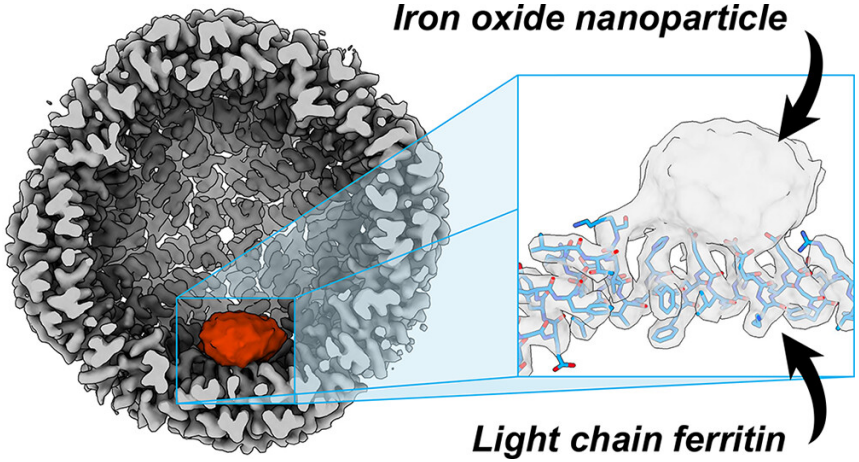

January 15, 2025

Why this paper ?

- Materials under biogenic confinement – bridges biology and materials science
- Single particle analysis (SPA) study of FeO NP inside largely stable protein
- Direction towards atomically precise nanoclusters clusters and protein conjugates

Apoferritin -1.96 Å

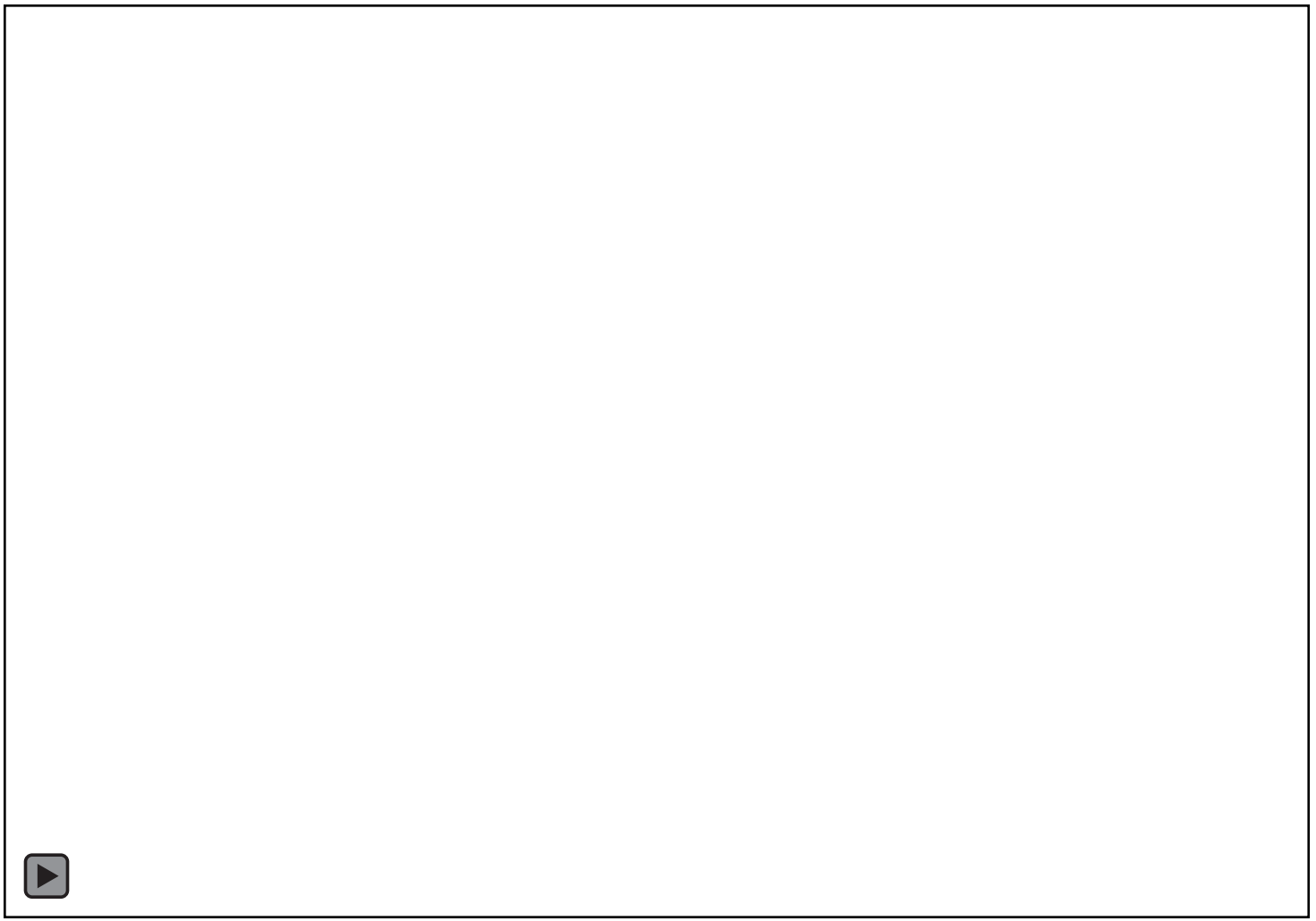

Where this NP will seat ???

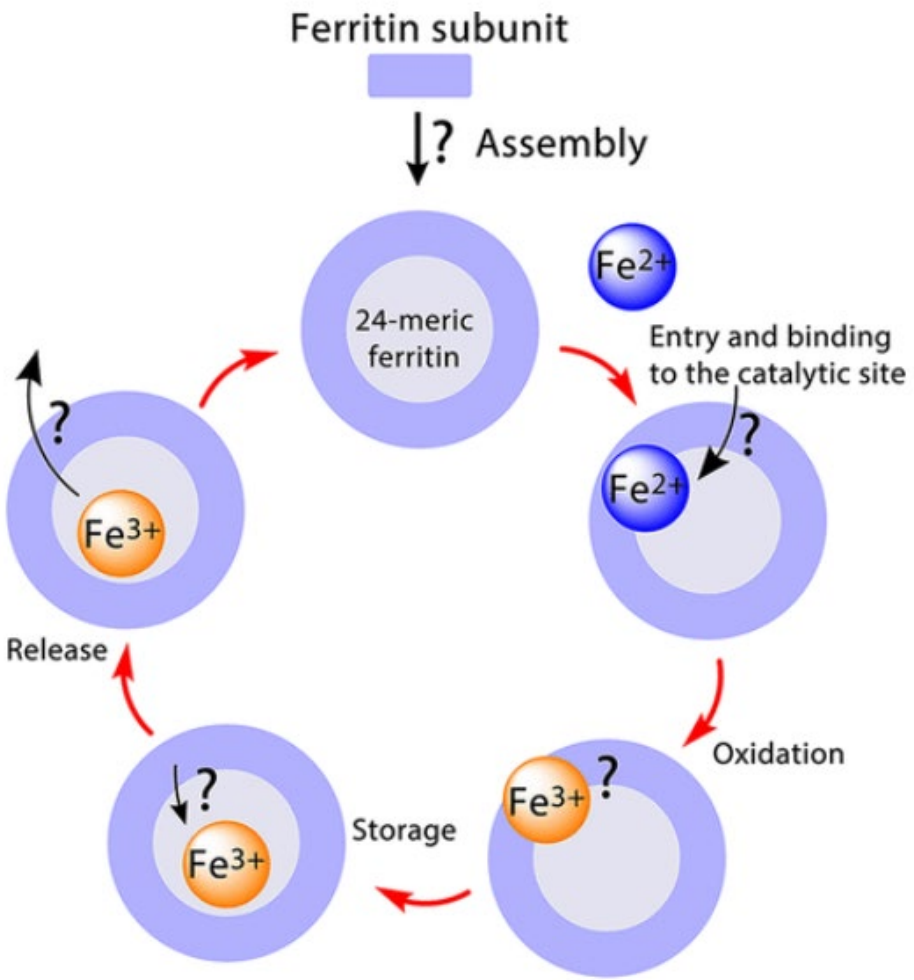

- Mechanism of functioning of ferritin is divided into six steps: (1) Assembly of subunits to form the 24-meric shell of ferritin, (2 and 3) entry of Fe(II) to ferritin and binding to catalytic centers, (4) oxidation of Fe(II) in the catalytic center, (5) storage of the Fe(III) product inside the cavity of ferritin, and (6) release of Fe(III) from the mineral core.

Honarmand Ebrahimi et al.,*Chem. Rev.* **2015**, *115*(1),295-326.

JACS
JOURNAL OF THE AMERICAN CHEMICAL SOCIETY
ACS AUTHORCHOICE
pubs.acs.org/JACS
Article

Folding of an Intrinsically Disordered Iron-Binding Peptide in Response to Sedimentation Revealed by Cryo-EM

Geula Davidov,[⊥] Gili Abelya,[⊥] Ran Zalk, Benjamin Izbicki, Sharon Shaibi, Lior Spektor, Dayana Shagidov, Esther G. Meyron-Holtz, Raz Zarivach, and Gabriel A. Frank*

Cite This: J. Am. Chem. Soc. 2020, 142, 19551−19557
Read Online

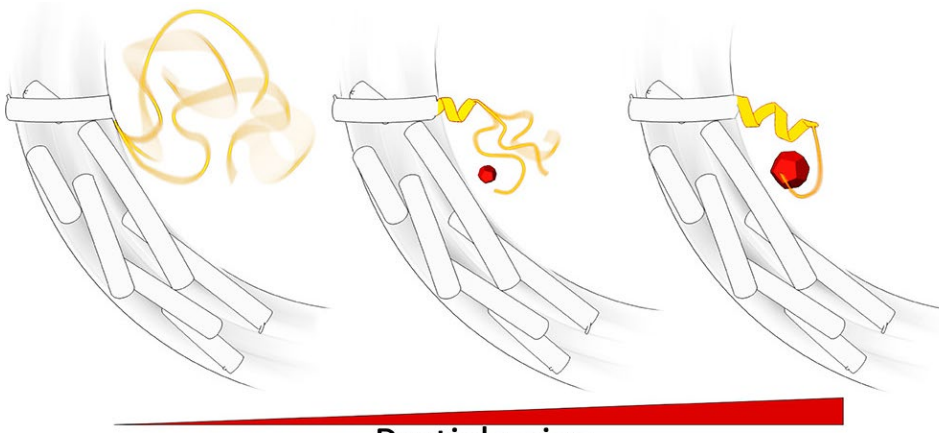

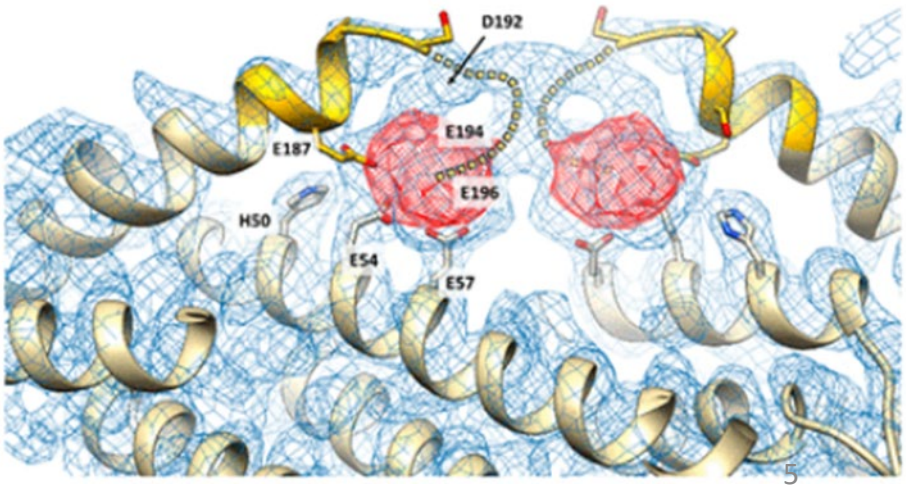

Structural Insights into Iron Ions Accumulation in Dps Nanocage

by Yury Chesnokov [1,2], Andrey Mozhaev [1,3,4,5], Roman Kamyshinsky [1,2,6], Alexander Gordienko [1,7] and Liubov Dadinova [1,*]

Int. J. Mol. Sci. **2022**, *23*(10), 5313

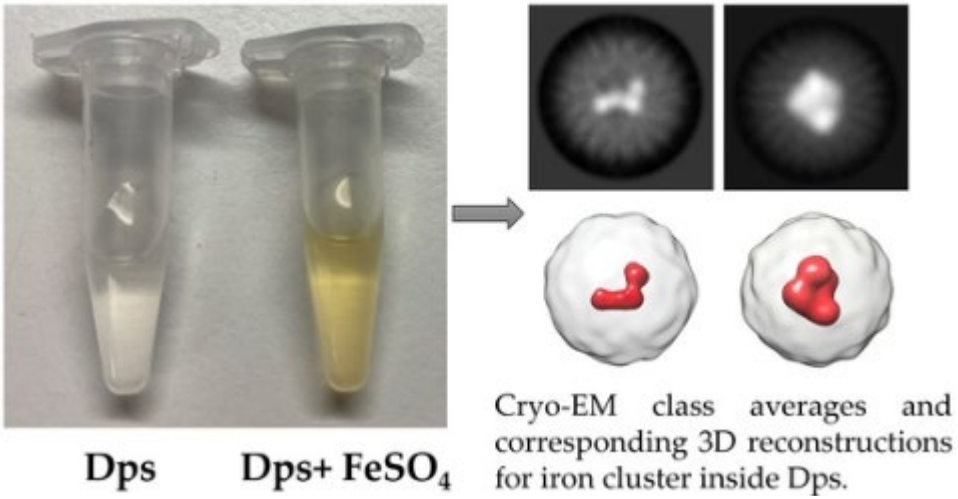

Cryo-EM class averages and corresponding 3D reconstructions for iron cluster inside Dps.

Results and Discussion

	HuLF-NP PDB ID 9bpj EMD-44777	**apo-HuLF** PDB ID 9bpk EMD-44780	**HuLF$_{\Delta 177\text{-}178}$ NP** PDB ID 9bpi EMD-44778	**apo-HuLF$_{\Delta 177\text{-}178}$** PDB ID 9bq5 EMD-44797
Data Collection and Processing				
Magnification	48,544	48,544	48,544	48,544
Voltage (kV)	300	300	300	300
Exposure ($e^-/Å^2$)	72.48	72.48	72.48	72.48
Defocus range (μm)	-0.8 to -2.6	-0.8 to -2.6	-0.8 to -2.6	-0.8 to -2.6
Pixel size (Å)	1.03	1.03	1.03	1.03
Symmetry	C1	O	C1	O
Final particle images	123,544	542,755	85,039	381,609
Map resolution (FSC = 0.143) (Å)	2.85	2.10	3.30	2.36

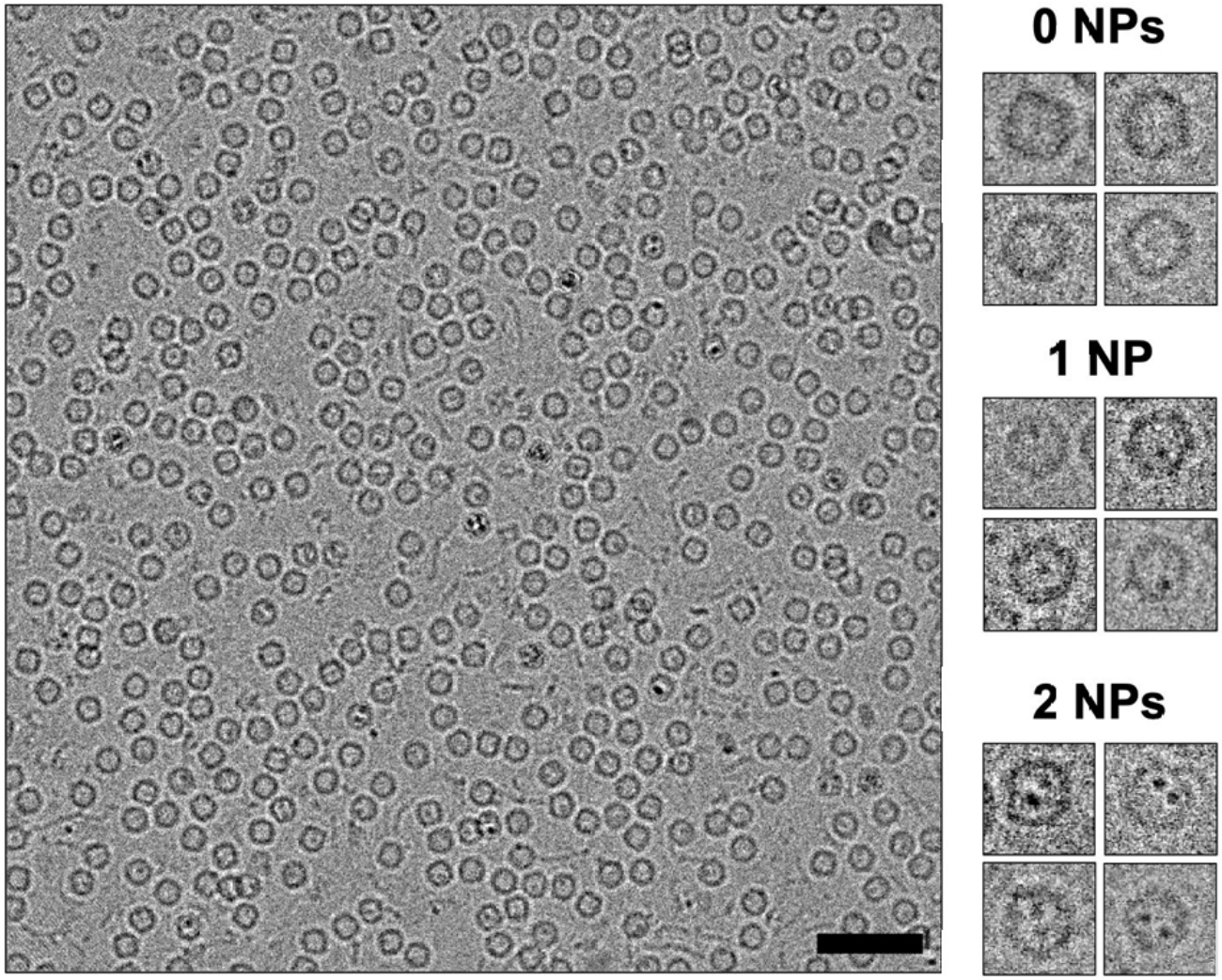

Fig. S1. Representative cryo-EM micrograph of iron oxide NP bound HuLF. Scale bar represents 50 nm. Example single particles from the data set with 0, 1, and 2 NPs.

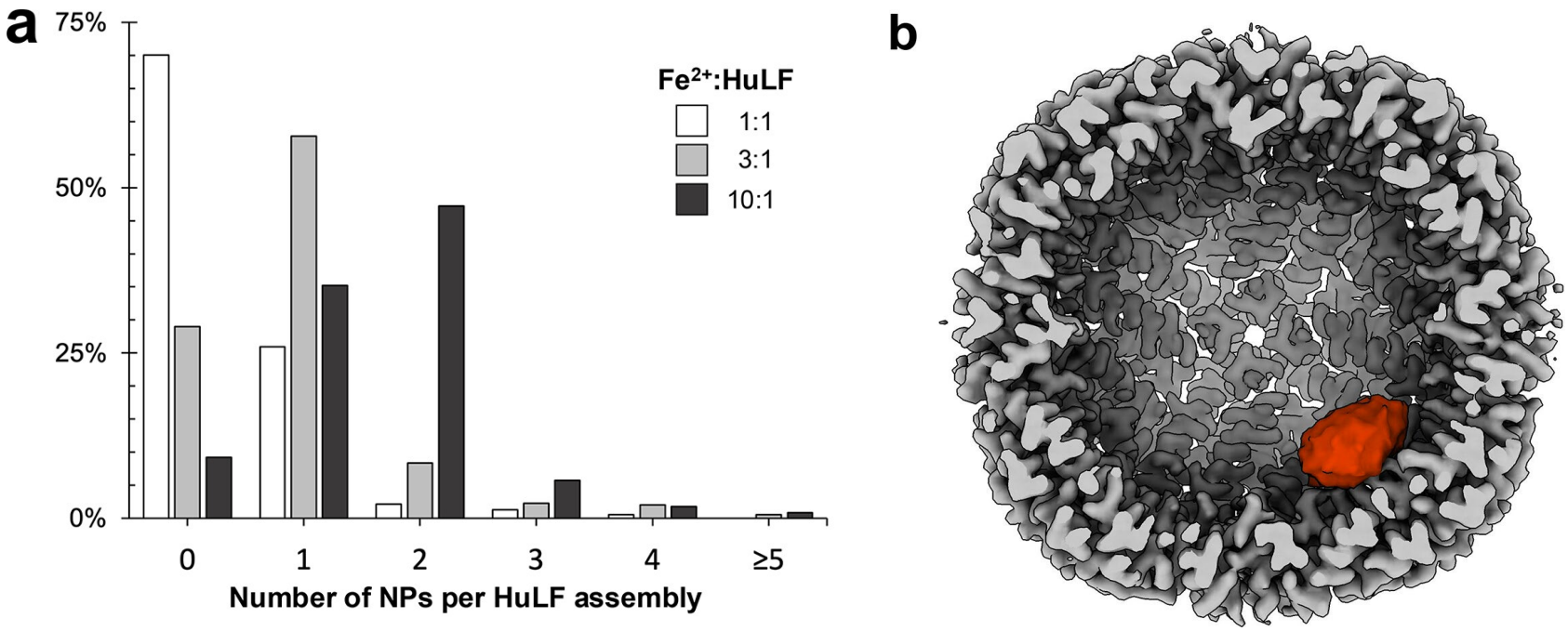

Figure 1. Synthesis and structure of iron oxide NP-bound HuLF. (a) The synthesis of NP-bound HuLF was optimized to produce the highest ratio of HuLF assemblies with a single NP. As Fe^{2+} was increased, the number of NPs per HuLF was increased with the optimal Fe^{2+}:HuLF ratio tested being 3:1. (b) Using the 3:1 ratio, single particle cryo-EM was used to determine the structure of HuLF bound to an iron oxide NP (HuLF-NP) at 2.85 Å, which was sufficient to resolve interactions of the interfacial amino acids.

Data processing workflow

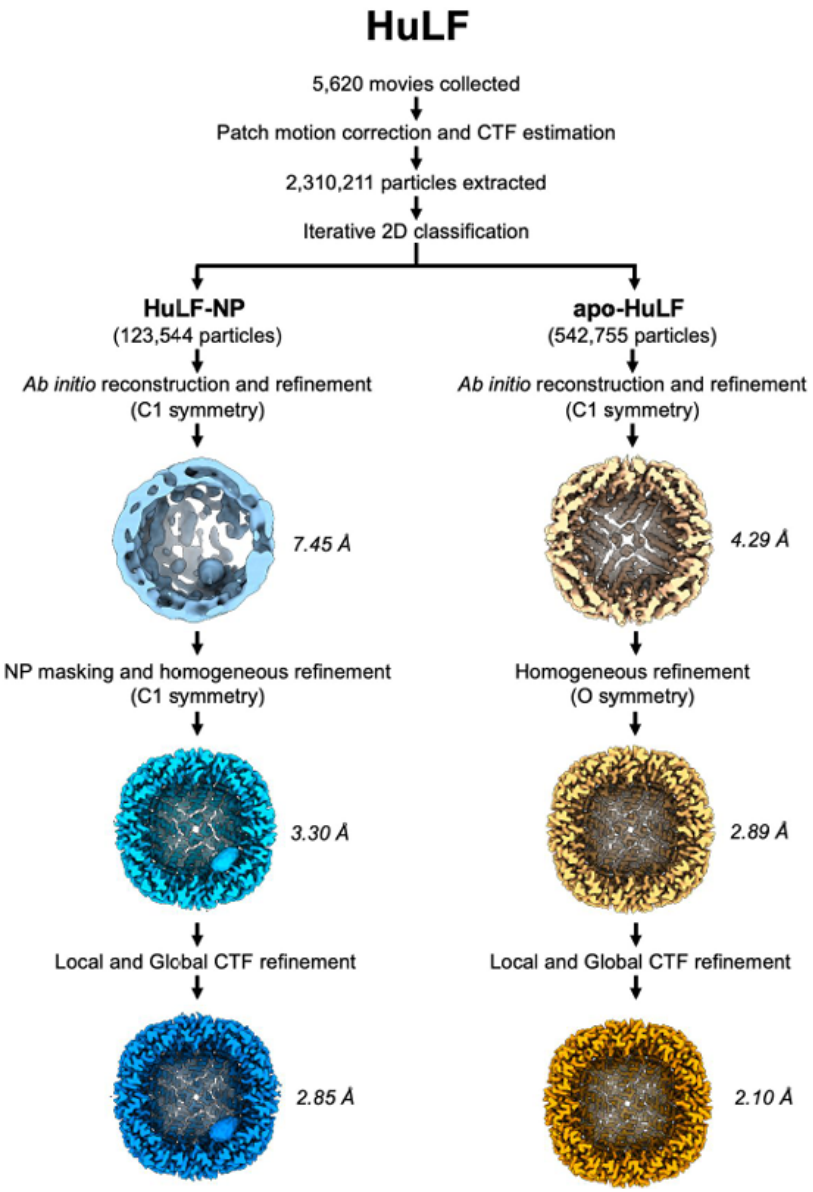

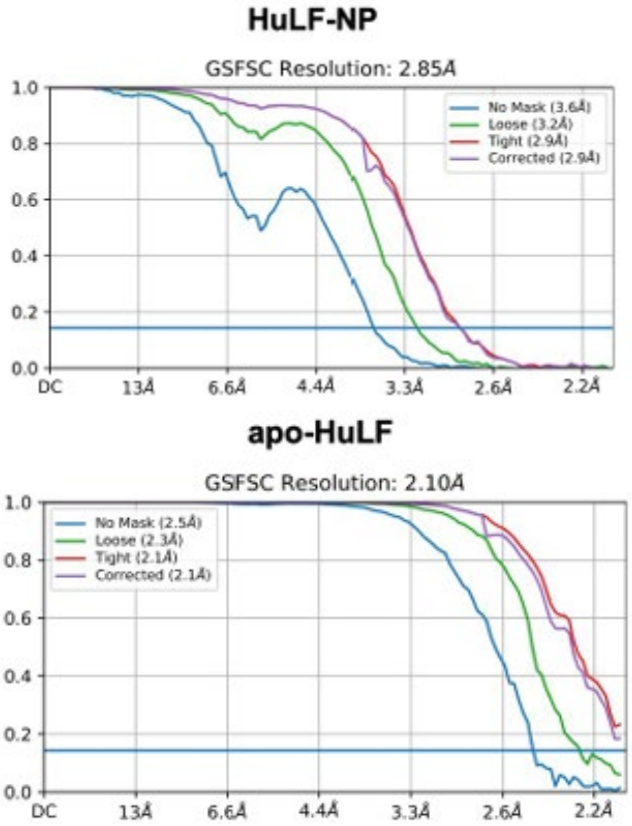

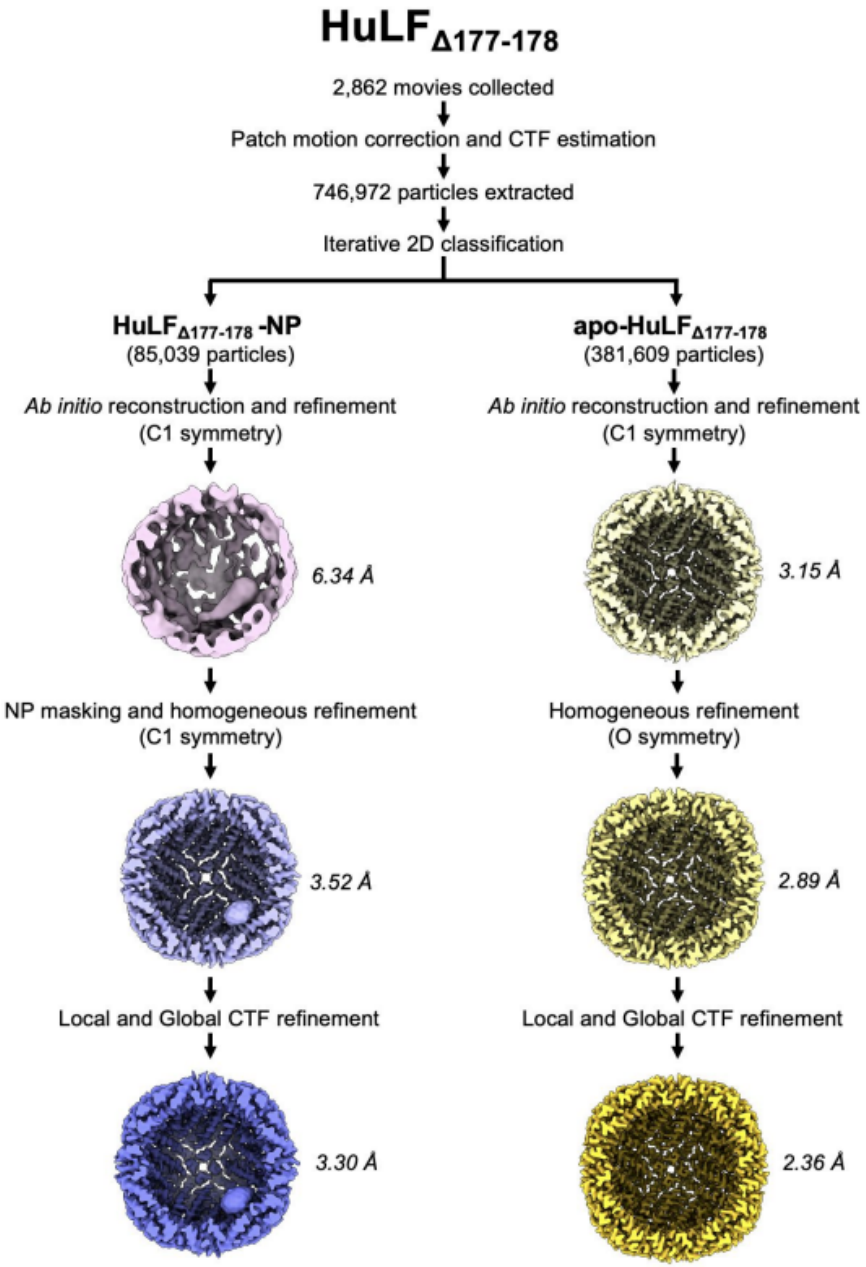
HuLF Δ177-178
2,862 movies collected
Patch motion correction and CTF estimation
746,972 particles extracted
Iterative 2D classification
HuLF Δ177-178 -NP
(85,039 particles)
apo-HuLF Δ177-178
(381,609 particles)
Ab initio reconstruction and refinement
(C1 symmetry)
Ab initio reconstruction and refinement
(C1 symmetry)
6.34 Å
3.15 Å
NP masking and homogeneous refinement
(C1 symmetry)
Homogeneous refinement
(O symmetry)
3.52 Å
2.89 Å
Local and Global CTF refinement
Local and Global CTF refinement
3.30 Å
2.36 Å

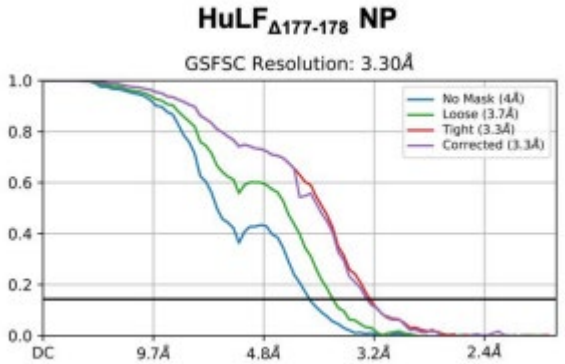
HuLF Δ177-178 NP
GSFSC Resolution: 3.30Å
No Mask (4Å)
Loose (3.7Å)
Tight (3.3Å)
Corrected (3.3Å)
1.0
0.8
0.6
0.4
0.2
0.0
DC
9.7Å
4.8Å
3.2Å
2.4Å

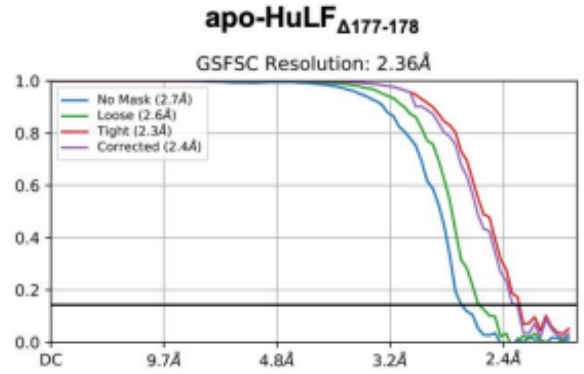
apo-HuLF Δ177-178
GSFSC Resolution: 2.36Å
No Mask (2.7Å)
Loose (2.6Å)
Tight (2.3Å)
Corrected (2.4Å)
1.0
0.8
0.6
0.4
0.2
0.0
DC
9.7Å
4.8Å
3.2Å
2.4Å

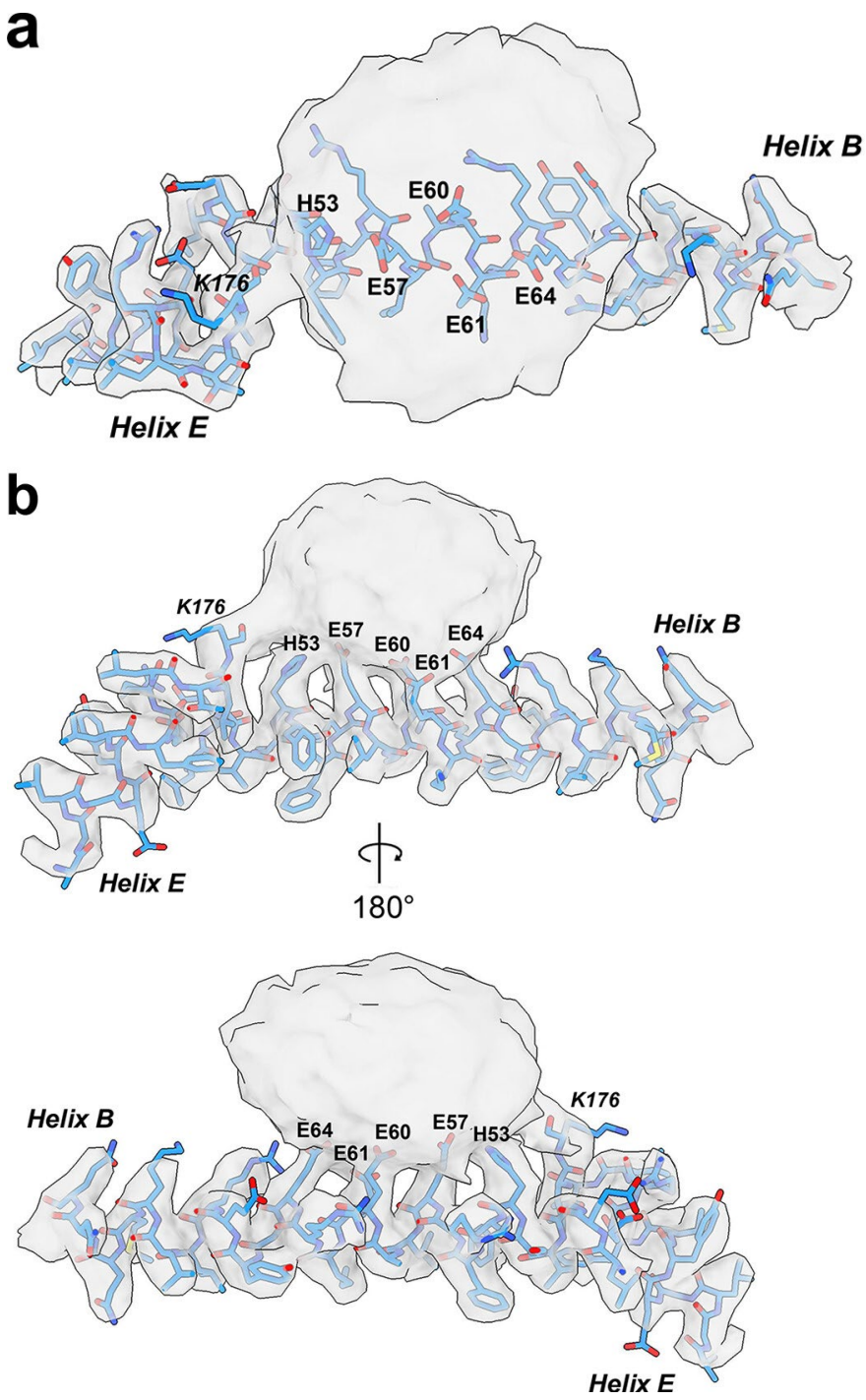

Figure 2. Cryo-EM structure of the protein-inorganic interface of HuLF. The 2.85 Å cryo-EM map and model of the HuLF-NP complex are shown from the top (a) and sides (b). The cryo-EM map is contoured at 5 σ around helix B and E of the HuLF-NP model, which is where the protein-inorganic interface is formed. The key residues in the interaction with helix B are labeled (H53, E57, E60, E61, and E64) as well as the interaction of the C-terminus, which follows helix E and is labeled with the last residue modeled, K176.

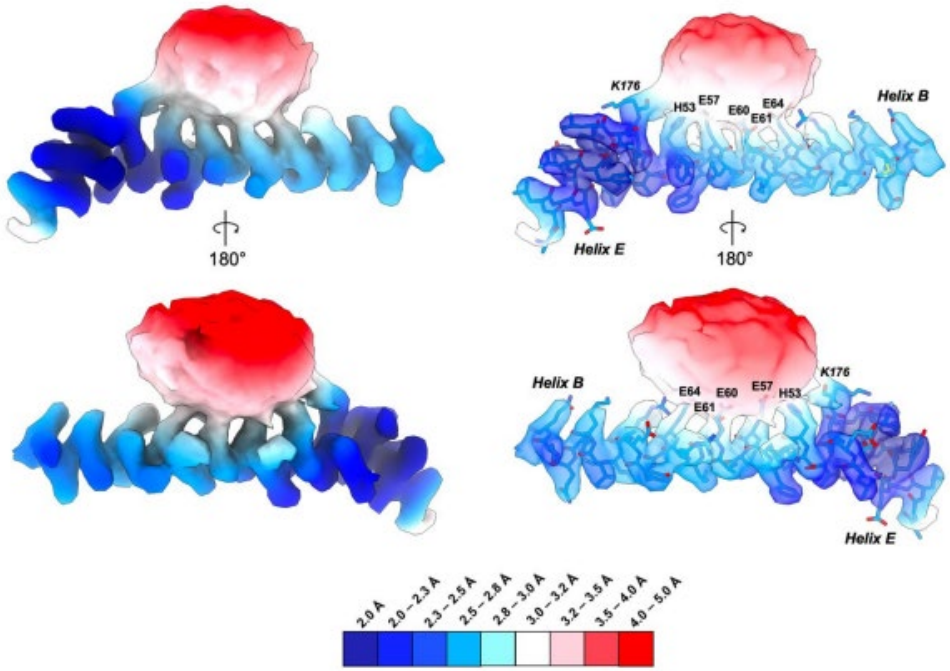

Fig. S5. Local resolution map around the protein-inorganic interface of HuLF-NP. Local resolution map was calculated using Phenix and visualized using ChimeraX.

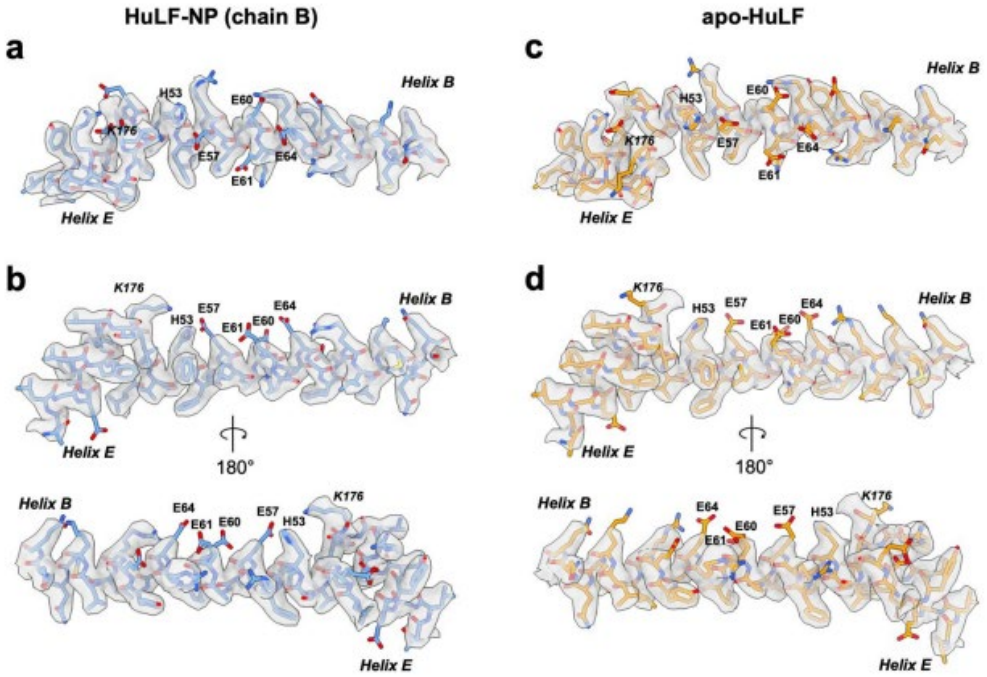

Fig. S6. Cryo-EM maps of HuLF not interacting with iron oxide NPs. (a-b) Top and side views of a representative chain (chain B) in the HuLF-NP structure that is not interacting with the NP (chain A). (c-d) Top and side views of apo-HuLF in the area that the NP would be bound (see Fig. 2). The structure of apo-HuLF is from the same data set used to determine HuLF-NP (see Fig. S2). Maps are contoured at 5.0σ.

Chemistry at the protein–mineral interface in L-ferritin assists the assembly of a functional (μ^3-oxo)Tris[(μ^2-peroxo)] triiron(III) cluster

Cecilia Pozzi, Silvia Ciambellotti, Caterina Bernacchioni, +2, and Paola Turano Authors Info & Affiliations

Edited by Harry B. Gray, California Institute of Technology, Pasadena, CA, and approved January 20, 2017 (received for review August 26, 2016)

February 15, 2017 | 114 (10) 2580-2585 | https://doi.org/10.1073/pnas.1614302114

E60 / E61 / E64 / E57

Iron Biomineral Growth from the Initial Nucleation Seed in L-Ferritin

Dr. Silvia Ciambellotti, Prof. Cecilia Pozzi, Prof. Stefano Mangani, Prof. Paola Turano

First published: 06 February 2020 | https://doi.org/10.1002/chem.202000064 | Citations: 23

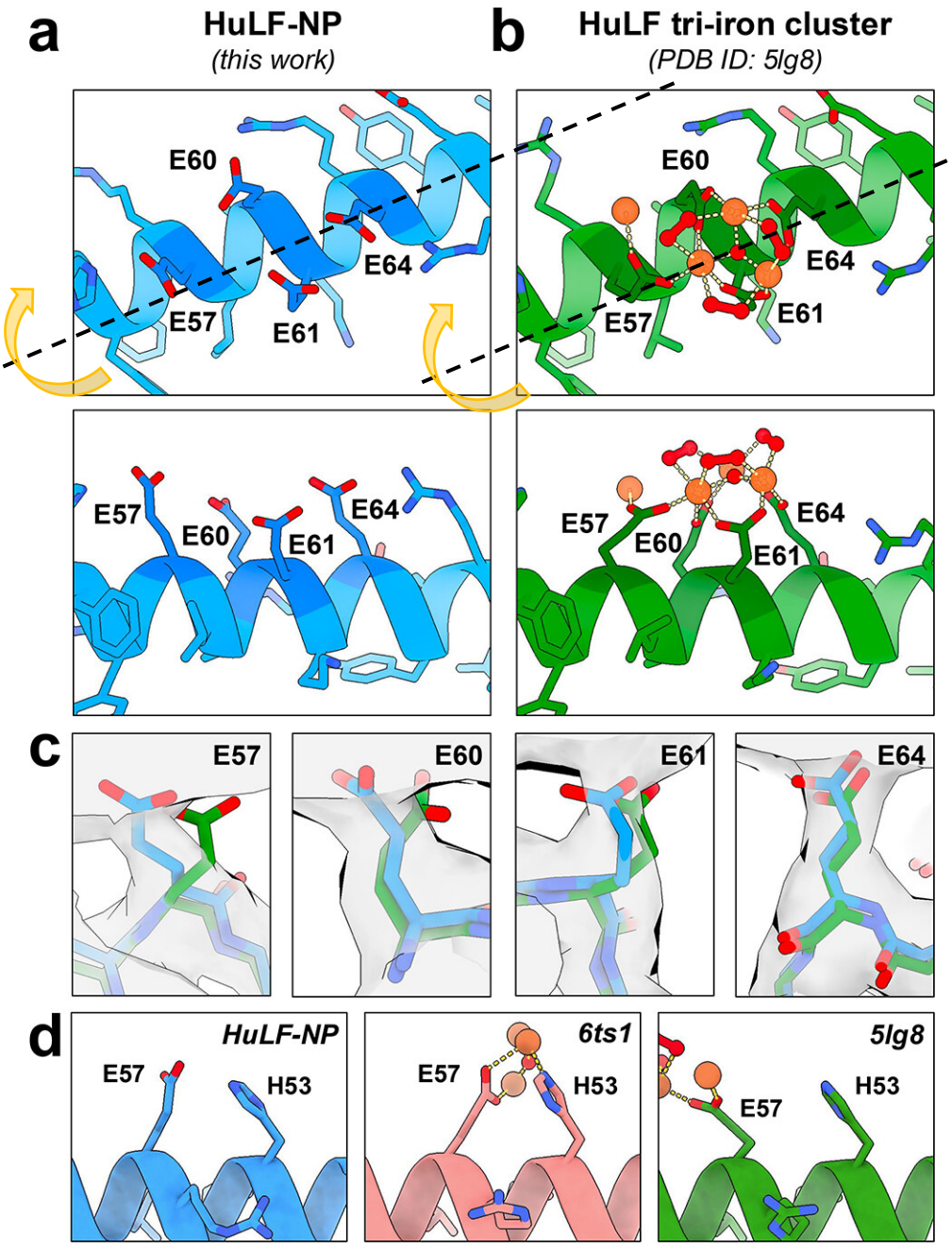

Figure 3. Comparison of the cryoEM HuLF-NP complex structure to the iron cluster structures determined by X-ray crystallography. The models derived from the cryo-EM maps of HuLF-NP determined in this work (a) show key differences when compared with the model of smaller tri-iron clusters by X-ray crystallography (b, PDB ID: 5lg8), particularly the conformations of E57 and E60 (c). (d) While there are significant differences between E57 in HuLF-NP (d, top) and the tri-iron cluster from PDB ID 5lg8 (d, bottom), the conformation of E57 in the HuLF-NP structure is much more similar to E57 from the E60A/E61A/E64A HuLF mutant that forms an alternative iron cluster (d, bottom. PDB ID: 6ts1). The HuLF-NP maps presented in (c) are contoured at 5 σ.

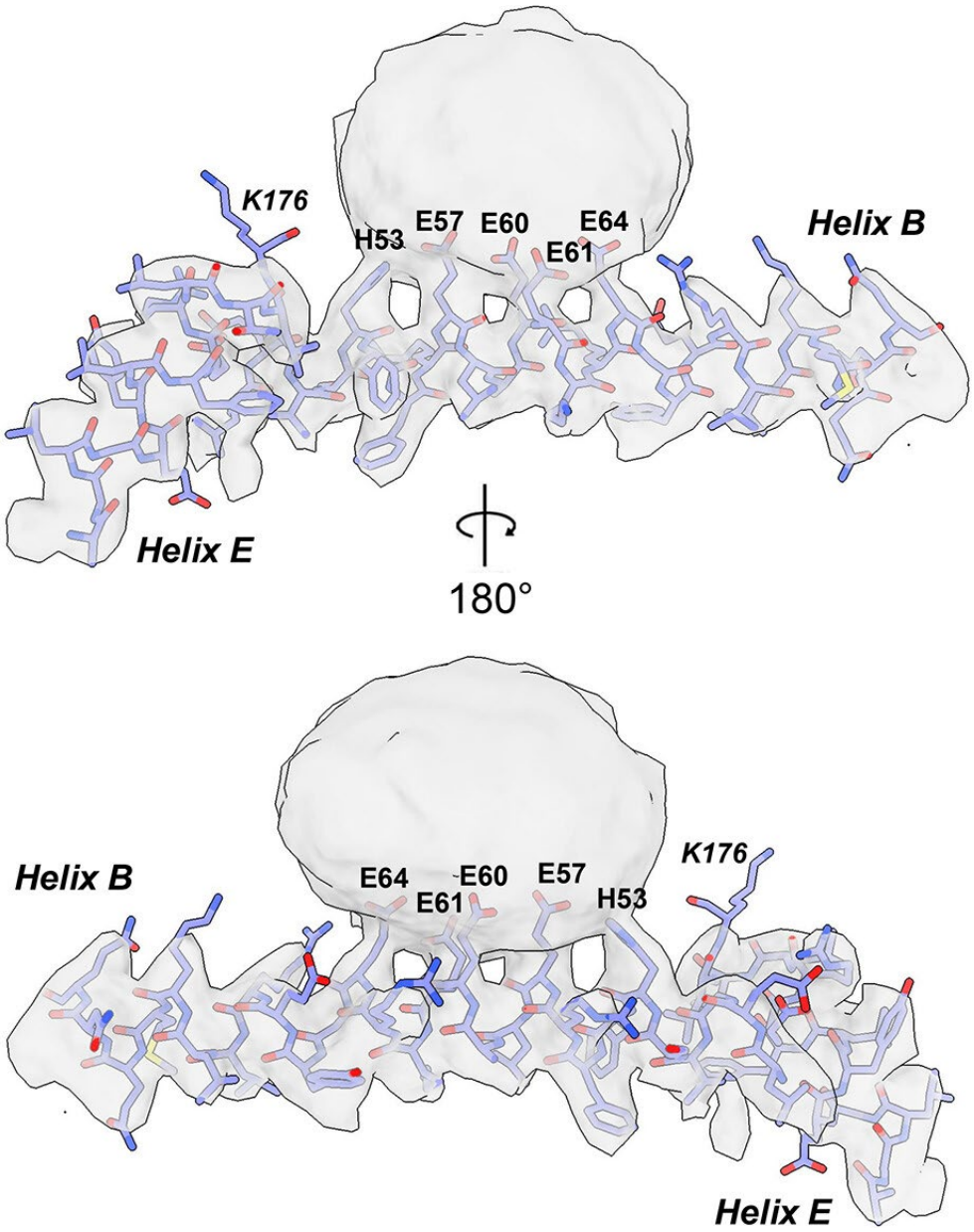

Figure 4. The cryo-EM structure of the NP-bound HuLF C-terminal truncated variant. The $HuLF_{\Delta 177–178}$ construct was used to produce a 3.30 Å cryo-EM map of the NP complex with HuLF lacking the final two residues, H177 and D178. The map is similar to the wild-type HuLF-NP structure, with the exception of the lack of continuous density from the C-terminus of $HuLF_{\Delta 177–178}$ to the NP. The cryo-EM map is contoured at 3.0 σ around helices B and E of chain A

Conclusions

- The cryo-EM structures of iron oxide NP-bound HuLF presented here provide a more complete view of the **protein-inorganic interface in ferritin**, complementing past studies and adding to our understanding of ferritin biomineralization.

- Single particlecryo-EM is capable of resolving high-resolution details at the protein-inorganic interface. The use of cryo-EM is an excellent complement to X-ray crystallography, as it alleviates many difficulties associated with using crystallography in biomineralizing proteins. For example, the mineralization conditions may not be compatible with the crystallization mother liquor, and as is the case for ferritin, extended incubations with mineralization precursors can degrade the crystal quality.
- The resulting cryo-EM maps confirmed and enhanced previously proposed interactions of the protein with the material along the B-helix and revealed new interaction at the C-terminus of light chain ferritin.